

# 4.45 Pflops Astrophysical $N$ -Body Simulation on K computer - The Gravitational Trillion-Body Problem

Tomoaki Ishiyama

Center for Computational Science  
University of Tsukuba  
ishiyama@ccs.tsukuba.ac.jp

Keigo Nitadori

Center for Computational Science  
University of Tsukuba  
keigo@ccs.tsukuba.ac.jp

Junichiro Makino

Graduate School of Science and Engineering  
Tokyo Institute of Technology  
makino@geo.titech.ac.jp

**Abstract**—As an entry for the 2012 Gordon-Bell performance prize, we report performance results of astrophysical  $N$ -body simulations of one trillion particles performed on the full system of K computer. This is the first gravitational trillion-body simulation in the world. We describe the scientific motivation, the numerical algorithm, the parallelization strategy, and the performance analysis. Unlike many previous Gordon-Bell prize winners that used the tree algorithm for astrophysical  $N$ -body simulations, we used the hybrid TreePM method, for similar level of accuracy in which the short-range force is calculated by the tree algorithm, and the long-range force is solved by the particle-mesh algorithm. We developed a highly-tuned gravity kernel for short-range forces, and a novel communication algorithm for long-range forces. The average performance on 24576 and 82944 nodes of K computer are 1.53 and 4.45 Pflops, which correspond to 49% and 42% of the peak speed.

## I. INTRODUCTION

Astrophysical  $N$ -body simulations have been widely used to study the nonlinear structure formation in the Universe. Such simulations are usually called as cosmological  $N$ -body simulations. In these simulations, a particle moves according to the gravitational forces from all the other particles in the system.

Thus, the most straightforward algorithm to calculate the acceleration of a particle is to calculate the  $N - 1$  forces from the rest of the system, where  $N$  is the total number of particles in the system. This method is usually called the direct summation. This method is unpractical for large  $N$  ( $N > 10^6$ ), since the calculation cost is proportional to  $N^2$ . Therefore, faster algorithms with some approximation are usually used in cosmological  $N$ -body simulations.

The tree algorithm [1] [2] is the most widely used algorithm for cosmological  $N$ -body simulations. The basic idea of the tree algorithm is to use a hierarchical oct-tree structure to represent an  $N$ -body system (figure 1). The force from particles in one box to one particle can be calculated by evaluating the multipole expansion, if the error is small enough (if the box and the particles are well separated). If not, the force is evaluated as the sum of forces from eight subboxes. By recursively applying this procedure, one can calculate the total force on a particle with  $\mathcal{O}(\log N)$  cost,

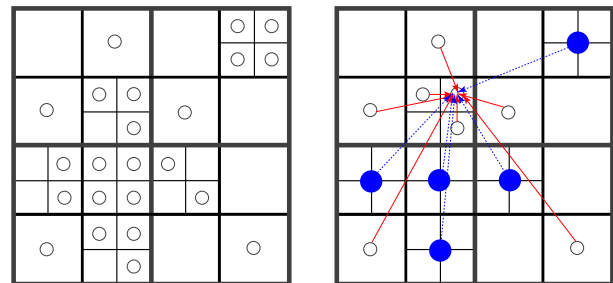


Fig. 1. The hierarchical tree algorithm. White circles represent particles. Blue circles are the multipole expansions of tree nodes. Red solid arrows and blue dotted arrows show the particle-particle and the particle-multipole interactions, respectively.

and the total calculation cost per timestep becomes  $\mathcal{O}(N \log N)$ , achieving drastic reduction from the  $\mathcal{O}(N^2)$  cost of the direct summation method.

Thus, the tree algorithm have been used for most of practical large cosmological calculations in the last two decades, and many Gordon-Bell prizes have been given to such simulations (1992 [3], 1995-2001 [4]–[10], 2003 [11], and 2009-2010 [12] [13]). In order to accelerate the calculation of gravity, some of them used GRAPEs [4] [5] [8]–[11], which are special-purpose computers [14]–[16], or graphics processing units (GPUs) [12] [13].

There is one difference between large cosmological simulations in the literature and those awarded Gordon-Bell prizes so far. In practically all recent large calculations, except for those for Gordon-Bell prizes, the periodic boundary condition is used. With the periodic boundary condition, the computational domain is a cube, and we assume that there are infinite copies of them which fill the infinite space. This condition is used to model the Universe which is uniform in very large scale. On the other hand, in simulations for past Gordon-Bell prizes, the open boundary condition, in which the calculation domain is initially a sphere, was used.

From theoretical point of view, in both cases one can only analyze structures of the size sufficiently small compared to the size of the computational domain. However, periodic boundary is computationally more efficient. The reason is that with open boundary, only the structures near the center of the sphere are reliable. Structures near the boundary are affected

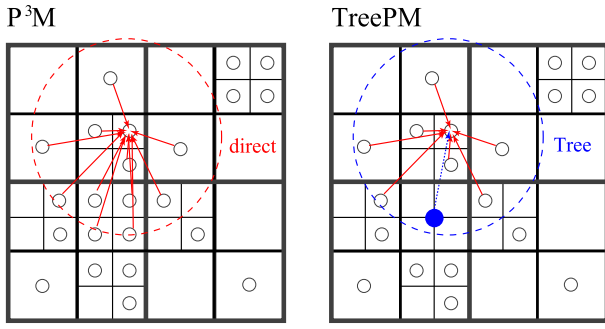


Fig. 2. The schematic view of the  $P^3M$  and the TreePM algorithm. Large red and blue dashed circles show the cutoff radius of each algorithm. Within these radii, the short-range forces are calculated by the direct method or the tree algorithm. White circles represent particles. Blue circles are the multipole expansions of tree nodes. Red solid arrows and blue dotted arrows show the particle-particle and the particle-multipole interactions, respectively. The residual force is calculated by the PM algorithm.

by the presence of the boundary to the vacuum. Thus, only a small fraction of the total computational volume is useful for the analysis of the structure formed. On the other hand, with the periodic boundary, everywhere is equally reliable and can be used for the analysis.

The PM (Particle Mesh) algorithm has been widely used in cosmological  $N$ -body simulations with the periodic boundary condition since 1980's. The PM algorithm can obtain the gravitational potential on a regular grid. The mass density at a grid point is calculated by assigning the masses of nearby particles by some kernel function. Then, the Poisson equation is solved using FFT. Finally, the gravitational force on a particle position is obtained by differentiating and interpolating the potential on the mesh. For details, see Eastwood (1981) [17].

In general, the PM algorithm is much faster but less accurate than the tree algorithm since the spatial force resolution is limited by the size of the mesh. In order to overcome this problem, hybrid algorithm such as the  $P^3M$  (Particle-Particle Particle-Mesh) and the TreePM (Tree Particle-Mesh) algorithm have been developed. The main idea of these algorithm is that the gravitational force is split into two components, short- and long-range forces. The short-range force decreases rapidly at large distance, and drops zero at a finite distance. This part with the cutoff function on the force shape is calculated by a high resolution algorithm, such as the direct summation ( $P^3M$ ) or the tree algorithm (TreePM) (e.g. [18]–[24]). The long-range force drops at large wavenumbers in the frequency space, and is calculated by the PM algorithm. Figure 2 shows a schematic view of the  $P^3M$  and the TreePM algorithm.

In the  $P^3M$  and TreePM algorithms, we can calculate the gravitational potential with high spatial resolution under the periodic boundary condition. In cosmological  $N$ -body simulations, structures with high density form rapidly from the small initial density fluctuations via the gravitational instability. It is not practical to use the  $P^3M$  algorithm since the computational cost of the short-range part increases rapidly as the formation proceeds. The calculation cost of a cell within the cutoff

radius with  $n$  particles is  $\mathcal{O}(n^2)$ . Thus, for a cell with 1000 times more particles than average, the cost is  $10^6$  times more expensive. The TreePM algorithm can solve this problem, since the calculation cost of such cell is  $\mathcal{O}(n \log n)$ . Thus, the TreePM algorithm is very efficient and is used in a number of recent large cosmological  $N$ -body simulations (e.g. [25] [26]).

The TreePM algorithm is relatively new. It became popular around 2000. Thus, it is not surprising that Gordon-Bell winners in 1990's used the pure tree algorithm. Advantage of the TreePM algorithm over the pure tree algorithm is twofold. The first one is, as we already noted, we can use entire volume for data analysis. The second one is that for the same level of accuracy, the TreePM algorithm requires significantly less operations. With the tree algorithm, the contributions of distant (large) cells dominate the error in the calculated force. With the TreePM algorithm, the contributions of distant particles are calculated using FFT. Thus, we can allow relatively moderate accuracy parameter for the tree part, resulting in considerable reduction in the computational cost.

In this paper, we describe our MPI/OpenMP hybrid TreePM implementation GreeM [24], which is a massively parallel TreePM code based on the implementation of Yoshikawa & Fukushima (2005) [23] for large cosmological  $N$ -body simulations, and present performance results of the largest gravitational  $N$ -body simulation that has ever been done in the world. We use one trillion dark matter particles to study the nonlinear evolution of the first dark matter structures in the early Universe. The numerical simulations were carried out on K computer at the RIKEN Advanced Institute for Computational Science, which is the world's fastest supercomputer at the time this paper is submitted. It consists of 82944 SPARC64 VIIIfx oct-core processors with the clock speed of 2.0 GHz (the total number of core is 663552) and 1.3PB of memory. The peak performance is 10.6 Pflops.

The scientific motivation of this simulation is to study the nature of dark matter particles, which is a long-standing problem in both astrophysics and particle physics. One candidate of the dark matter particle is the lightest supersymmetric particle, the neutralino. Since the neutralino is itself its anti-particle, it self-annihilates and produces new particles and gamma-rays. Indirect detection experiments to detect these productions are the important way to study the nature of dark matter. Therefore, such indirect detection experiments are one of the key projects of the current generation gamma-ray space telescope Fermi [27] and the next generation ground-based cherenkov telescope array CTA<sup>1</sup>.

The Milky Way is in the bottom of the potential of a dark matter halo, which is ten times larger than the Milky Way itself. For precise predictions of the annihilation gamma-rays in the Milky Way, we need to know the fine structures of dark matter halos, since the gamma-ray flux from dark matter structures is proportional to the square of their density and inverse square of the distance from us. Ishiyama et al. (2010) [28] found that the central density of the smallest dark

<sup>1</sup><http://www.cta-observatory.org/>

matter structures is very high. If they survive near our Sun, the annihilation signals could be observable as gamma-ray point-sources. Thus, the behavior of the smallest dark matter structures near Sun is very important for the indirect detection experiments.

The cosmological  $N$ -body simulation is useful for the study of the structure and evolution of dark matter structures within the Milky Way. Analytical studies (e.g. [29] [30]) predicted the mass of the smallest structures to be comparable to the mass of the earth, which is 18 orders of magnitude smaller than that of the Milky Way. Unfortunately, we cannot simulate such a wide dynamic range with currently available computational resources. Ishiyama et al. 2010 [28] simulated only the smallest structures. With the simulation described here, we extend this strategy further. We simulate a much larger volume than that used in Ishiyama et al. 2010 [28], and study the evolution. Using these results, we can predict their evolution of the smallest structures survive or not near Sun.

This paper is organized as follows. First, we describe our parallel TreePM implementation. Then we present the detail of the simulation with one trillion particles and report the performance of our code on K computer.

## II. OUR PARALLEL TREEPM CODE

In the TreePM method, the force on a particle is divided into two components, the long-range (PM) part and the short-range (PP: particle-particle) part. The long-range part is evaluated by FFT, and the short-range part is calculated by the tree method, with a cutoff function on the force shape. The density of point mass  $m$  is decomposed into PM part and PP part:

$$\rho_{\text{PM}}(r) = \begin{cases} \frac{3m}{\pi} \left( \frac{2}{r_{\text{cut}}} \right)^3 \left( 1 - \frac{r}{r_{\text{cut}}/2} \right), & (0 \leq r \leq r_{\text{cut}}/2), \\ 0, & (r > r_{\text{cut}}/2), \end{cases} \quad (1)$$

$$\rho_{\text{PP}}(r) = \frac{m}{4\pi} \delta^3(r) - \rho_{\text{PM}}(r).$$

The function  $\rho_{\text{PM}}$  expresses a linearly decreasing density (shape S2) [17]. Since  $4\pi \int_0^{r_{\text{cut}}/2} r^2 \rho_{\text{PM}}(r) dr = m$  and  $4\pi \int_0^{r_{\text{cut}}/2} r^2 \rho_{\text{PP}}(r) dr = 0$ , the particle-particle interaction vanishes outside the finite radius  $r_{\text{cut}}$  (Newton's second theorem). We use a small softening with length  $\varepsilon \ll r_{\text{cut}}$  to the short-range interaction that corresponds to replacing the delta function with a small kernel function.

Given the positions  $\mathbf{r}_i$ , the masses  $m_i$  and the gravitational constant  $G$ , the particle-particle interaction takes the form

$$\mathbf{f}_i = \sum_{j \neq i}^N G m_j \frac{\mathbf{r}_j - \mathbf{r}_i}{|\mathbf{r}_j - \mathbf{r}_i|^3} g_{\text{P3M}}(2|\mathbf{r}_j - \mathbf{r}_i|/r_{\text{cut}}). \quad (2)$$

The cutoff function  $g_{\text{P3M}}$  is obtained by evaluating the force between two particles with the density of equation (1) by six-

dimensional spatial integration,

$$g_{\text{P3M}}(\xi) = \begin{cases} 1 + \xi^3 \left( -\frac{8}{5} + \xi^2 \left( \frac{8}{5} + \xi \left( -\frac{1}{2} + \xi \left( -\frac{12}{35} + \xi \frac{3}{20} \right) \right) \right) \right) \\ - \zeta^6 \left( \frac{3}{35} + \xi \left( \frac{18}{35} + \xi \frac{1}{5} \right) \right), & (0 \leq \xi \leq 2), \\ \text{where } \zeta = \max(0, \xi - 1), \\ 0, & (\xi > 2). \end{cases} \quad (3)$$

Here, we modified the original form [17] with a branch at  $\xi = 1$ , which is optimized for the evaluation on a SIMD (Single Instruction Multiple Data) hardware with FMA (Fused Multiply-Add) support.

For the tree part, we used Barnes' modified algorithm [2] in which the traversal of the tree structure is done for a group of particles. It is done for each particle in the original algorithm [1]. In the modified algorithm, a list of tree nodes and particles are shared by a group of particles. The forces from nodes and particles in the list to particles in groups are calculated directly. This modified algorithm can reduce the computational cost of tree traversal by a factor of  $\langle N_i \rangle$ , where  $\langle N_i \rangle$  is the average number of particles in groups. On the other hand, the computational cost for the PP force calculation increases since the interactions between particles in groups are calculated directly, and the average length of the interaction list becomes longer. The optimal value of  $\langle N_i \rangle$  depends on the performance characteristics of the computer used. It is around 100 for K computer, and 500 for a GPU cluster [12].

We use a 3-D multi-section decomposition [31]. As a result, the shape of a domain is rectangular. We use the sampling method [32] to determine the geometries of domains. The sampling method allows us to drastically reduce the amount of communication needed for constructing the division because we use only a small subset of particles. It is difficult to achieve good load balance for the following reason. In cosmological  $N$ -body simulations, the initial particle distribution is close to uniform with small density fluctuations. These fluctuations grow nonlinearly via the gravitational instability and form a number of high density dark matter structures in the simulation box. The density of such structures are typically a hundred or a thousand times higher than the average. Sometimes, the central density of these structures can reach  $\sim 10^7$  times the average. In such a situation, the calculation cost of the short-range part becomes highly imbalanced, if the domain decomposition is static, in other words, its geometry of each domain is time invariable and is the same for all domains.

In our method, we adjust the geometries of the domains assigned to individual processes, so that the total calculation time of the force (sum of the short-range and long-range forces) becomes the same for all MPI processes. We achieve this good load balance by adjusting the sampling rate of particles in one domain according to their calculation costs. We adjust the sampling rate of particles in one domain so that it is proportional to the measured calculation time of the short-range and long-range forces. Thus, if the calculation time of a process is larger than the average value, the number of sampled particles of the process becomes relatively larger. After the root

process gathers all sampled particles from the others, the new domain decomposition is created so that all domains have the same number of sampled particles. Therefore, the size of the domain for this process becomes somewhat smaller, and the calculation time for the next timestep is expected to become smaller.

Figure 3 shows the domain decomposition for a cosmological simulation. We can see that high density structures are divided into small domains so that the calculation costs of all processes are the same.

We update the geometries every step following the evolution of the simulated system. The cost is negligible compared to the effect of the load imbalance. However, often large jumps of boundaries occur since there are fluctuations due to sampling. In order to avoid the large jumps of the boundaries, we adopt the linear weighted moving average technique for boundaries of last five steps. Thus, we suppress sudden increment of the amount of transfer of particles across boundaries.

The detailed explanation of the GreeM code can be found in Ishiyama et al. (2009) [24]. In the rest of this section, we describe two novel techniques that significantly improved the performance. The first is the near-ultimate optimization of the equation (3). The second is the relay mesh method for the PM part.

#### A. Optimized Particle-Particle Force Loop

Most of the CPU time is spent for the evaluation of the particle-particle interactions. Therefore we have developed a highly optimized loop for that part. This force loop was originally developed for the x86 architecture with the SSE instruction set, and named Phantom-GRAPe [33]–[35] after its API compatibility to GRAPe-5 [36]. We have ported Phantom-GRAPe with support for the cut-off function (eq.3) to the HPC-ACE architecture of K computer.

The LINPACK peak per core of SPARC64 XIIIfx is 16 Gflops (4 FMA units running at 2.0 GHz). However, the theoretical upper limit of our force loop is 12 Gflops because it consists of 17 FMA and 17 non-FMA operations ( $51 \times 2$  floating-point operations in total)<sup>2</sup> for two (one SIMD) interactions. Our force loop reaches 11.65 Gflops on a simple  $\mathcal{O}(N^2)$  kernel benchmark, which is 97% of the theoretical limit.

We have implemented the force loop with SIMD built-in functions provided by the Fujitsu C++ compiler which define various operations on a packed data-type of two double-precision numbers. The loop was unrolled eight times by hand so that 16 pairwise interactions, forces from 4-particles to 4-particles are evaluated in one iteration. Furthermore the loop was ten-times unrolled and software-pipelined by the compiler.

An inverse-square-root was calculated using a fast approximate instruction of HPC-ACE with 8-bit accuracy and a third-order convergence method with  $y_0 \sim 1/\sqrt{x}$ ,  $h_0 = 1 - xy_0^2$ ,  $y_1 = y_0(1 + \frac{1}{2}h_0 + \frac{3}{8}h_0^2)$  to obtain 24-bit accuracy. A

<sup>2</sup> 17 fmadd/fmsub/fnmadd/fnmsub, 9 fmul, 4 fadd/fsub, 3 fmax/fcmp/fand, and 1 frsqrrta.

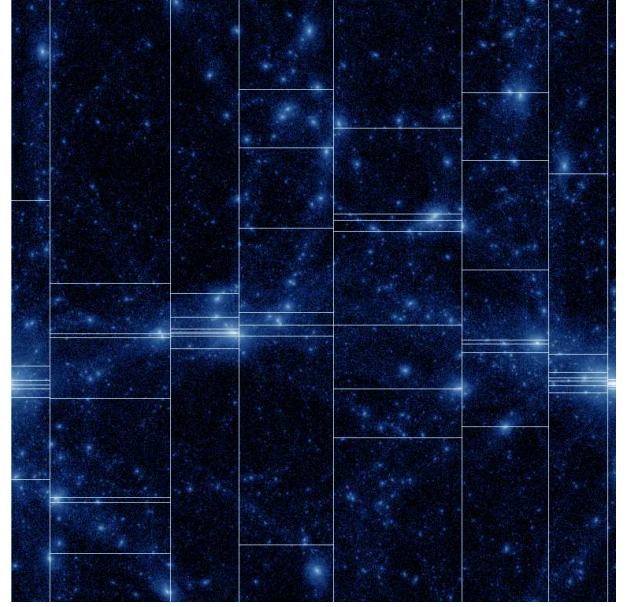


Fig. 3. The example of the domain decomposition. It shows  $8 \times 8$  division in two dimensions.

full convergence to double-precision will increase both CPU time and the flops count, without improving the accuracy of scientific results.

#### B. Relay Mesh Method

For the parallel FFT of the PM part, we use the MPI version of the FFTW 3.3 library<sup>3</sup>. The data layout supported by the parallel FFTW is the 1-D slab decomposition only. The drawback of this 1-D parallel FFT is that the number of processes that perform FFT is limited by the number of grid point of the PM part in one dimension. We usually use the number of PM mesh  $N_{PM}$  between  $N/2^3$  and  $N/4^3$  in order to minimize the force error [24]. If we perform a  $10240^3$  particles simulation, the number of mesh is between  $2560^3$  and  $5120^3$ . Consequently, the number of processes perform FFT is  $2560 \sim 5120$ , which is very small fraction of the total number of cores of K computer. When we perform parallel FFT via `MPI_COMM_WORLD`, FFTW allocates processes to perform FFT in ascending order of their ranks in the communicator `MPI_COMM_WORLD`. In this case, processes with their ranks  $0 \sim 2559$  or  $0 \sim 5119$  perform FFT. The others with larger ranks do not perform FFT. Usually, it is not clear how an MPI rank corresponds to the physical layout of a node. Thus, when the number of processes is larger than the number of grid point in one dimension, if we use `MPI_COMM_WORLD`, the communication pattern within the FFT processes is likely to be not optimized. In order to avoid this problem, we select processes to perform FFT so that their physical positions are close to one another and create a new communicator `COMM_FFT` by calling `MPI_Comm_split`, which includes these processes only.

<sup>3</sup><http://www.fftw.org/>



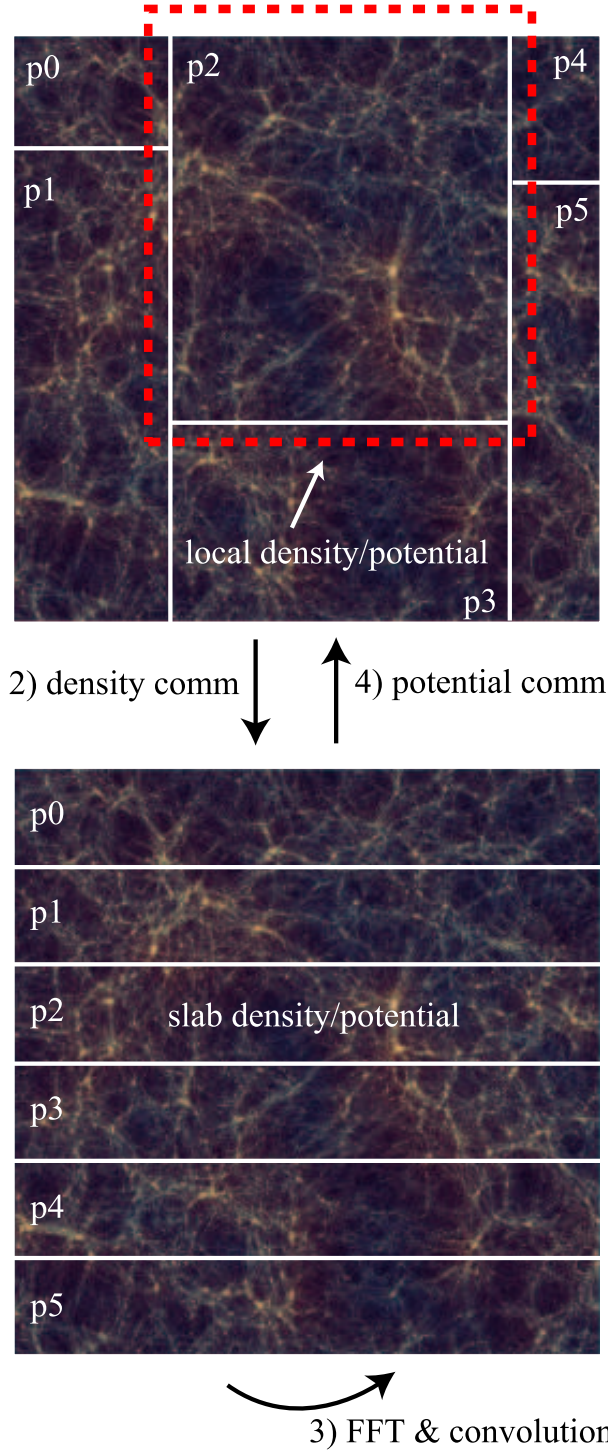


Fig. 4. Two domain decompositions for the PM method. Upper panel shows the domain decomposition of local mesh structures. Bottom panel shows the domain decomposition of slab mesh structures for the parallel FFT. In this figure, p[0-5] mean the identification number of each process. The local mesh of a process covers only own domain but contains some ghost layer which is needed according to an adopted interpolation scheme for the density assignment and the calculation of forces on particle positions.

In the following, we first describe a straightforward implementation and its limitation. Then we describe our solution.

The 1-D parallel FFT requires the conversion of data layout in order to perform the 1-D parallel FFT. Particles are distributed in 3-D domain decomposition in our parallelization method for the optimization of the load balance. This means that optimal domain decompositions are quite different for the particles and the PM mesh. However, the conversion of the data layout of particles would be heavy task since almost all particles have to be exchanged. The best way to perform the conversion is to exchange the mass density on the mesh after the assignment of the mass of all particles to the local mesh. After the assignment, a process has the mesh that covers only its own domain. Then, each process communicates the local mesh so that the FFT processes receive the complete slabs. After the calculation of the potential on the mesh is completed, we perform the conversion of the 1-D distributed potential slabs to the 3-D distributed rectangular mesh for the calculation of forces. Figure 4 shows an illustration of two different domain decompositions for the PM method.

In GreeM, a cycle of the parallel PM method proceeds in the following five steps.

- 1) Each process calculates the mass density on the local mesh by assigning the mass of all particles using the TSC (Triangular Shaped Cloud) scheme, where a particle interacts with 27 grid points. The mesh of each process covers only its own domain.
- 2) The FFT processes construct the slab mesh by incorporating the contributions of the particles in other processes. Each process sends the density of the local mesh to other processes by calling `MPI_Alltoallv(..., MPI_COMM_WORLD)`<sup>4</sup>. Each FFT process receives and sums up only the contributions that overlap with their own slabs from other processes.
- 3) Then the gravitational potential on the slabs are calculated by using the parallel FFT (via `COMM_FFT`) and performing the convolution with the Green's function of the long-range force.
- 4) The FFT processes send the gravitational potential on the slabs to all other processes by calling `MPI_Alltoallv(..., MPI_COMM_WORLD)`. Each process receives the contributions that cover its own local mesh from the FFT processes.
- 5) Each process has the gravitational potential on the local mesh that covers the domain of own process. The gravitational forces on the local mesh are calculated by the four point finite difference algorithm from the potential. Then we calculate the PM forces on particles by interpolating forces on the local mesh.

Since the calculation cost of FFT is relatively small in most cases, this 1-D parallel FFT does not cause significant degradation of the performance. However, in the situation that the number of MPI processes is very large, communication becomes problematic since the number of processes that

<sup>4</sup> One may imagine replacing this communication with `MPI_Isend` and `MPI_Irecv`. However, a FFT process receives meshes from  $\sim 4000$  processes. Such a large number of non-blocking communications do not work concurrently.

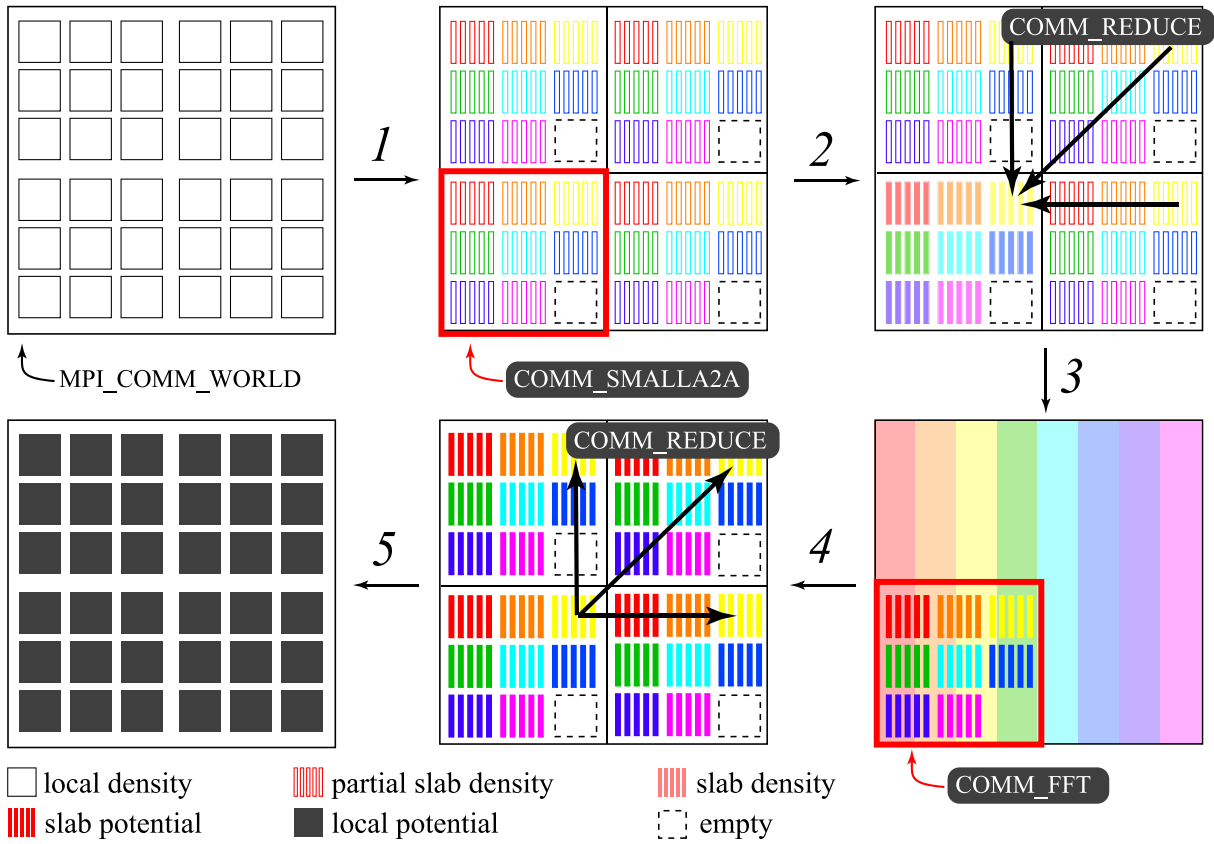


Fig. 5. Illustration of our communication algorithm, relay mesh method. There are 2-D decomposed  $6 \times 6$  processes. The number of the PM mesh is  $N_{PM} = 8^3$ , and that of processes perform FFT is eight. There are four groups that include nine processes. The detail explanation is written in the text. The background of bottom-right panel shows the physical regions that are corresponding to the slab density of each process in the root group.

send the local mesh to an FFT process is proportional to  $p^{2/3}$ , where  $p$  is the number of MPI processes. When we use 82944 processes, an FFT process receives slabs from  $\sim 4000$  processes, and network congestion would occur on the communication network. Thus, the communication time of the conversion of the mesh structures can become bottlenecks on modern massively parallel environments such as the full system of K computer.

In order to solve this problem, we developed a novel communication algorithm, *Relay Mesh Method*. The basic idea of this method is to split the global all-to-all communication on the conversion of the mesh structures into two local communication. Processes are divided into small groups whose sizes are equal or larger than that of the FFT processes. One of the groups contains the FFT processes, we call this group the root group. For example, consider a simulation with 2-D decomposed  $6 \times 6$  processes and  $N_{PM} = 8^3$ . In this case, the number of FFT processes is eight since the FFT is parallelized for only one axis. We make four groups that consist of  $3 \times 3 = 9$  processes. The eight processes of the root group perform FFT. The 1-D slab decomposed density mesh is constructed in the following two steps. First, each group compute the contribution of its particles to the mesh, and then the total mesh is constructed by adding up the contributions

from all groups. the global communication in the second step (previous page) is replaced by two local communications, one within groups and the other over groups. The first communication is done to construct the 1-D distributed density mesh in the same way as the second step of the original method, but the communication is closed within each group. In this example, the nine processes of each group send the mass density to eight processes within the same group. After the first communication, each group has the 1-D distributed partial density slabs. Then, all groups *relay* the partial slabs to the root group, and the root group reduces them to construct the complete slabs. In this example, four processes in different groups communicate. Figure 5 shows a schematic view of this method.

In order to perform these two communication steps, we create two communicators *COMM\_SMALLA2A* and *COMM\_REDUCE* by calling *MPI\_Comm\_split*.

- *COMM\_SMALLA2A* : Each process in a group can communicate with each other through this communicator (showed in the small red box in figure 5). One of group includes FFT processes (the root group).
- *COMM\_REDUCE* : Each process can communicate with processes in other groups with the same rank in the communicator *COMM\_SMALLA2A* (showed in same colors in

figure 5). The number of processes in this communicator is same as the number of groups.

In the case of the example showed in figure 5, the number of groups is four, and that of processes in each group is nine. Eight processes of the root group perform FFT. The number of communicator *COMM\_REDUCE* is eight, in which there are four processes.

The PM procedures 2-4 explained early in this subsection are replaced by following five steps (the numbers correspond to that in figure 5).

- 1) After the density assignment, each process sends the density of the local mesh to other processes in its group by calling `MPI_Alltoallv(..., COMM_SMALLA2A)`. In the case of figure 5, the 3-D distributed local mesh of nine processes are communicated to eight processes as the latter has the 1-D distributed partial density slabs.
- 2) Each process sends the slabs to the corresponding process in the root group by using `MPI_Reduce(..., COMM_REDUCE)`. After this communication, each process of the root group has the 1-D distributed complete slabs.
- 3) In the FFT processes, the gravitational potential on the slabs are calculated by using parallel FFT (via *COMM\_FFT*). The processes in other groups wait the end of FFT.
- 4) The root group sends the slab potential to other groups by means of `MPI_Bcast(..., COMM_REDUCE)` so that each group has the 1-D distributed complete slab potential.
- 5) Each process sends the gravitational potential on the slabs to other processes in the group by calling `MPI_Alltoallv(..., COMM_SMALLA2A)`. In the case of figure 5, the 1-D distributed slab potential of eight processes are communicated to nine processes.

Using this method, we can reduce network congestion. Here we present the timing result for  $4096^3$  FFT on 12288 nodes. If we do not use this method, the communication times for the conversion of the 3-D distributed local density mesh to the 1-D distributed density slabs and backward potential conversion were  $\sim 10$  and  $\sim 3$  seconds, respectively. With this method using three groups, these are reduced to  $\sim 3$  and  $\sim 0.3$  seconds. Thanks to our novel communication algorithm, we achieve speed up more than a factor of four for the communication. On the other hand, the calculation time of FFT itself was  $\sim 4$  seconds. Thus, FFT became a bottleneck after the optimization of these communication parts.

One might think a 3-D parallel FFT library will improve the performance further. A 3-D parallel FFT library requires that geometries of 3-D distributed density mesh in each process are the same for all processes. However, it is not practical to use similar geometries for the domain decomposition of the particles and the mesh in order to achieve good load balance. Thus, the communication with the conversion of a 3-D distributed rectangular mesh to a 3-D distributed regular

mesh is needed and is likely to be more complicated task than that of the combination of the 1-D parallel FFT and relay mesh method since we have to consider additional two axes. Although of course we consider to use such a library in the near future, this novel technique should be also applicable for the simplification of the conversion.

### III. COSMOLOGICAL $N$ -BODY SIMULATION

#### A. Calculation Setup

We performed cosmological  $N$ -body simulations of  $10240^3 (= 1,073,741,824,000)$  dark matter particles on 24576 and 82944 nodes. The latter is the full system of K computer. This is the largest cosmological  $N$ -body simulation has ever been done and is the first gravitational trillion body simulation in the world. The total amount of memory required is  $\sim 200$  TB. The number of PM mesh was  $N_{\text{PM}} = 4096^3$ . The cutoff radius for the short-range force  $r_{\text{cut}}$  are set to  $r_{\text{cut}} = 3/N_{\text{PM}}^{1/3} \sim 7.32 \times 10^{-4}$ , where the side length of the simulation box is unity.

For the parallelization, the number of divisions on each dimension is the same as that of physical nodes of K computer. These are  $32 \times 54 \times 48$  ( $32 \times 24 \times 32$ ) for the run on 82944 (24576) nodes. The number of divisions for the FFT processes is  $16 \times 16 \times 16$  ( $16 \times 8 \times 32$ ), the number of groups for relay mesh method is 18 (6).

We use a cube of the comoving size of 600 parsecs. The corresponding mass resolution is  $7.5 \times 10^{-12}$  solar masses. The smallest dark matter structures are represented by more than  $\sim 100,000$  particles. The initial condition was constructed as positions and velocities of particles represent the initial dark matter density fluctuations with the power spectrum containing a sharp cutoff generated by the free motion of dark matter particle (neutralino) with a mass of 100 GeV [37]. The cosmological parameters adopted are based on the concordance cosmological model [38].

In this project, we focus on the dynamics of the smallest dark matter structures at early Universe. We integrate the particle motion from redshift 400 to  $\sim 31$ . For the time integration, we adopted the multiple stepsize method [39] [40]. The one simulation step was composed by a cycle of the PM and two cycles of the PP and the domain decomposition. Figure 6 shows the snapshots of the simulation with 16.8G particles.

#### B. Performance

At the time of writing, the simulation is still running on 24576 nodes of K Computer (corresponds to  $\sim 30\%$  of the full system). We had an opportunity to measure the performance using the full system for only a limited time. The number of particle-particle interactions per step averaged in the last five steps is  $\sim 5.3 \times 10^{15}$ . The calculation time per step is 173.8 and 60.2 seconds for 24576 and 82944 nodes, respectively. Thus, the average performance on 24576 and 82944 nodes are 1.53 and 4.45 Pflops. The latter is  $\sim 1.44$  times higher than that of the Gordon-Bell peak performance winner of last year [41]. Here, we use the operation count of 51 per interaction



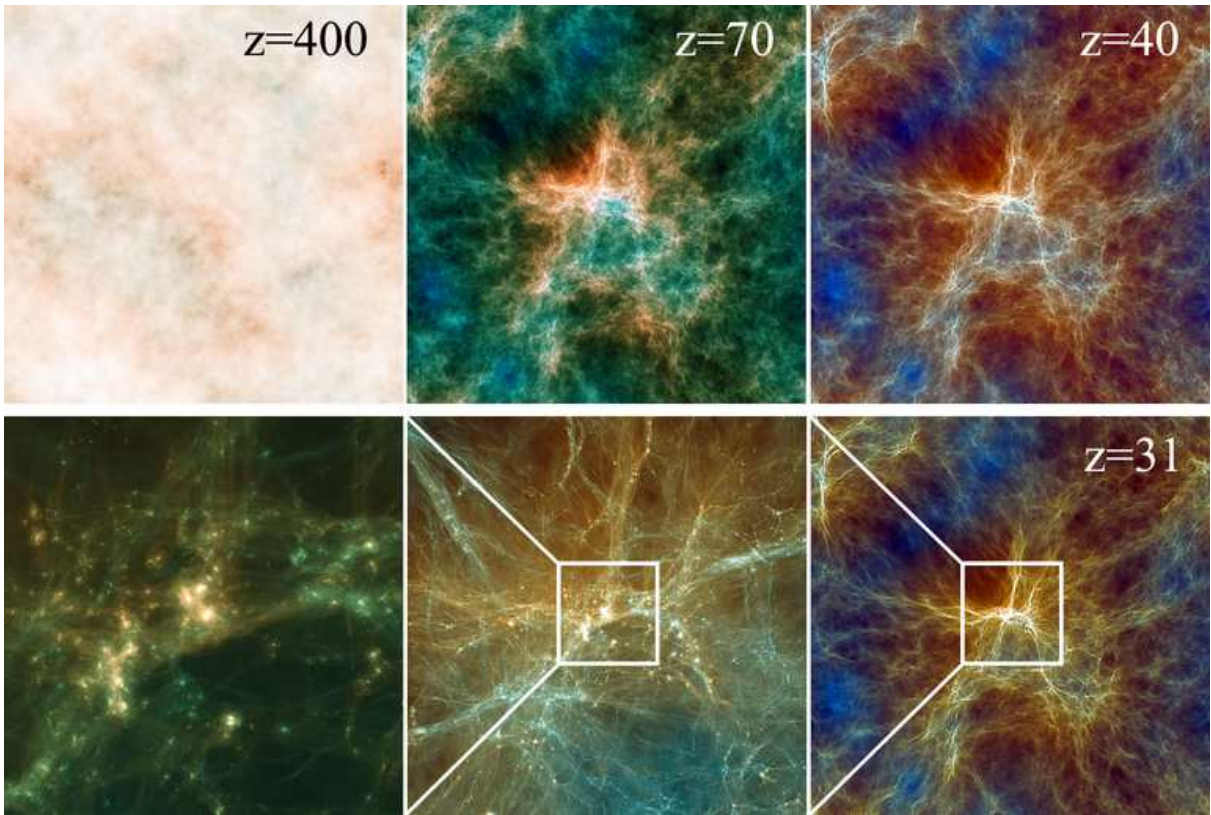


Fig. 6. The distribution of dark matter of the 16.8G particles simulation at redshift 400 (initial), 70, 40, and 31. The width of each image corresponds to 600 comoving parsecs. Bottom-left and bottom-middle images are enlargements of the image of  $z = 31$ . The sizes correspond to 37.5 (bottom-left) and 150 (bottom-middle) comoving parsecs.

following the description in subsection II-A. The measured efficiency reaches 49 and 42%. It is important to keep in mind that the performance is underestimated since we use only the particle-particle interaction part to estimate the performance. The performance analysis with the Fujitsu sampling profiler shows the efficiency a few percent higher since it counts all floating-point operations.

Table I gives the breakdown of the calculation cost per step, and the performance statistics. We can see that the short-range part achieves near ideal load balance. If we focus on the only force calculation cycle, it achieves 71% efficiency. As seen in subsection II-A, this value is equivalent to 95% efficiency since the theoretically maximum efficiency is 75%. On the other hand, the long-range part shows load imbalance since FFT is parallelized for only one axis. The number of the FFT processes was 4096, which is smaller than that of all processes we used. As a result, the calculation cost of FFT is the same in the simulations on 24576 and 82944 nodes. However, since the calculation cost of the long-range part is minimized by our novel relay mesh method, the high performance and excellent scalability is achieved even with the simulation on 82944 nodes.

Note that the average length of the interaction list ( $\langle N_j \rangle \sim 2000$ ) is about 6 times smaller than that of the previous Gordon-Bell winner who used a GPU cluster [12]. There

are two reasons for this difference. The first reason is the difference of the boundary condition. Hamada et al. (2009) adopted the open boundary condition, and used the tree algorithm for the entire simulation box. On the other hand, we adopted the periodic boundary condition and used the PM algorithm for the long-range force. The  $\log N$  term for our simulation is smaller than that of Hamada et al. (2009) because of the cutoff. The second reason is that they used large group size to achieve high performance on a PC with GPU. The optimal value of  $\langle N_i \rangle$  is around  $\sim 100$  for K computer, and  $\sim 500$  for GPU cluster [12].

#### IV. CONCLUSION

We present the performance results of the gravitational trillion-body problem on the full system of K computer. This is the largest astrophysical  $N$ -body simulation and is the first gravitational  $N$ -body simulation with one trillion particles. This simulation is a milestone that helps us to address the nature of the dark matter particles, which is one of the long-standing problem in astrophysics and particle physics.

The average performance achieved is 4.45 Pflops, which is 1.44 times higher than that of the Gordon-Bell peak performance winner of last year [41]. The efficiency of the entire calculation reaches 42%. The efficiency of the gravity kernel is 72%. These high efficiency is achieved by a highly optimized



TABLE I

CALCULATION COST OF EACH PART PER STEP AND THE PERFORMANCE STATISTICS. ONE STEP IS COMPOSED BY A CYCLE OF PM (LONG-RANGE PART) AND TWO CYCLES OF PP (SHORT-RANGE PART) AND DOMAIN DECOMPOSITION. WE USED  $N = 10240^3$  PARTICLES.

$p$ (#nodes)	24576	82944
$N/p$	43690666	12945382
PM(sec/step)	9.28	6.74
density assignment	1.44	0.44
communication	2.01	1.50
FFT	4.06	4.17
acceleration on mesh	0.13	0.13
force interpolation	1.64	0.50
PP(sec/step)	152.10	45.82
local tree	4.00	1.26
communication	3.70	2.02
tree construction	3.82	1.52
tree traversal	17.17	4.60
force calculation	122.18	35.72
Domain Decomposition(sec/step)	6.28	5.38
position update	0.28	0.08
sampling method	2.94	3.80
particle exchange	3.06	1.50
Total(sec/step)	173.84	60.20
$\langle N_i \rangle$	115	116
$\langle N_j \rangle$	2346	2328
#interactions/step	5.35 Peta	5.30 Peta
measured performance	1.53 Pflops	4.45 Pflops
efficiency	48.7%	42.0%

gravity kernel for short-range force calculation on the HPC-ACE architecture of K computer and by developing a novel communication algorithm for the calculation of long-range forces. Our implementation enables us to perform gravitational  $N$ -body simulations of one-trillion particles within practical time.

We will further continue the optimization of our TreePM code. The current bottleneck is FFT. We believe that the combination of our novel relay mesh method and a 3-D parallel FFT library will significantly improve the performance and the scalability. We aim to achieve peak performance higher than 5 Pflops on the full system of K computer.

#### ACKNOWLEDGMENT

We thank RIKEN Next-Generation Supercomputer R&D Center and Fujitsu Japan at the RIKEN AICS (Advanced Institute for Computational Science) for their generous support. Part of the results is obtained by early access to the K computer at the RIKEN AICS. K computer is under construction, the performance results presented in this paper are tentative. The early development of our simulation code was partially carried out on Cray XT4 at Center for Computational Astrophysics, CfCA, of National Astronomical Observatory of Japan. This work has been funded by MEXT HPCI STRATEGIC PROGRAM.

#### REFERENCES

- [1] J. Barnes and P. Hut, "A hierarchical  $O(N \log N)$  force-calculation algorithm," *Nature*, vol. 324, pp. 446–449, Dec. 1986.
- [2] J. E. Barnes, "A Modified Tree Code Don't Laugh: It Runs," *Journal of Computational Physics*, vol. 87, pp. 161–, Mar. 1990.
- [3] M. S. Warren and J. K. Salmon, "Astrophysical n-body simulations using hierarchical tree data structures," in *Proceedings of the 1992 ACM/IEEE conference on Supercomputing*, ser. Supercomputing '92. Los Alamitos, CA, USA: IEEE Computer Society Press, 1992, pp. 570–576. [Online]. Available: <http://dl.acm.org/citation.cfm?id=147877.148090>
- [4] J. Makino and M. Taiji, "Astrophysical n-body simulations on grape-4 special-purpose computer," in *Proceedings of the 1995 ACM/IEEE conference on Supercomputing (CDROM)*, ser. Supercomputing '95. New York, NY, USA: ACM, 1995. [Online]. Available: <http://doi.acm.org/10.1145/224170.224400>
- [5] T. Fukushige and J. Makino, "N-body simulation of galaxy formation on grape-4 special-purpose computer," in *Proceedings of the 1996 ACM/IEEE conference on Supercomputing (CDROM)*, ser. Supercomputing '96. Washington, DC, USA: IEEE Computer Society, 1996. [Online]. Available: <http://dx.doi.org/10.1145/369028.369130>
- [6] M. S. Warren, J. K. Salmon, D. J. Becker, M. P. Goda, T. Sterling, and G. S. Winckelmans, "Pentium pro inside: I. a treecode at 430 gigaflops on asci red, ii. price/performance of \$50/mflop on loki and hyglac," vol. 0. Los Alamitos, CA, USA: IEEE Computer Society, 1997, p. 61.
- [7] M. S. Warren, T. C. Germann, P. S. Lomdahl, D. M. Beazley, and J. K. Salmon, "Avalon: an alpha/linux cluster achieves 10 gflops for \$15k," in *Proceedings of the 1998 ACM/IEEE conference on Supercomputing (CDROM)*, ser. Supercomputing '98. Washington, DC, USA: IEEE Computer Society, 1998, pp. 1–11. [Online]. Available: <http://dl.acm.org/citation.cfm?id=509058.509130>
- [8] A. Kawai, T. Fukushige, and J. Makino, "\$7.0/mflops astrophysical n-body simulation with treecode on grape-5," in *Proceedings of the 1999 ACM/IEEE conference on Supercomputing (CDROM)*, ser. Supercomputing '99. New York, NY, USA: ACM, 1999. [Online]. Available: <http://doi.acm.org/10.1145/331532.331598>
- [9] J. Makino, T. Fukushige, and M. Koga, "A 1.349 tflops simulation of black holes in a galactic center on grape-6," in *Proceedings of the 2000 ACM/IEEE conference on Supercomputing (CDROM)*, ser. Supercomputing '00. Washington, DC, USA: IEEE Computer Society, 2000. [Online]. Available: <http://dl.acm.org/citation.cfm?id=370049.370426>
- [10] J. Makino and T. Fukushige, "A 11.55 tflops simulation of black holes in a galactic center on grape-6," in *Proceedings of the 2001 ACM/IEEE conference on Supercomputing (CDROM)*, ser. Supercomputing '01, 2001.
- [11] J. Makino, E. Kokubo, and T. Fukushige, "Performance evaluation and tuning of grape-6 - towards 40 "real" tflops," in *Proceedings of the 2003 ACM/IEEE conference on Supercomputing*, ser. SC '03. New York, NY, USA: ACM, 2003, pp. 2–. [Online]. Available: <http://doi.acm.org/10.1145/1048935.1050153>
- [12] T. Hamada, T. Narumi, R. Yokota, K. Yasuoka, K. Nitadori, and M. Taiji, "42 tflops hierarchical n-body simulations on gpus with applications in both astrophysics and turbulence," in *Proceedings of the Conference on High Performance Computing Networking, Storage and Analysis*, ser. SC '09. New York, NY, USA: ACM, 2009, pp. 62:1–62:12. [Online]. Available: <http://doi.acm.org/10.1145/1654059.1654123>
- [13] T. Hamada and K. Nitadori, "190 tflops astrophysical n-body simulation on a cluster of gpus," in *Proceedings of the 2010 ACM/IEEE International Conference for High Performance Computing, Networking, Storage and Analysis*, ser. SC '10. Washington, DC, USA: IEEE Computer Society, 2010, pp. 1–9. [Online]. Available: <http://dx.doi.org/10.1109/SC.2010.1>
- [14] D. Sugimoto, Y. Chikada, J. Makino, T. Ito, T. Ebisuzaki, and M. Umemura, "A special-purpose computer for gravitational many-body problems," *Nature*, vol. 345, pp. 33–35, May 1990.
- [15] J. Makino and M. Taiji, *Scientific Simulations with Special-Purpose Computers—the GRAPE Systems*, M. Makino, J. & Taiji, Ed., Apr. 1998.
- [16] J. Makino, T. Fukushige, M. Koga, and K. Namura, "GRAPE-6: Massively-Parallel Special-Purpose Computer for Astrophysical Particle Simulations," *Publ. of the Astron. Society of Japan*, vol. 55, pp. 1163–1187, Dec. 2003.

- [17] R. W. Hockney and J. W. Eastwood, *Computer Simulation Using Particles* (New York: McGraw-Hill), J. W. Hockney, R. W. & Eastwood, Ed., 1981.
- [18] G. Xu, "A New Parallel N-Body Gravity Solver: TPM," *Astrophys. J. Supp.*, vol. 98, pp. 355–, May 1995.
- [19] P. Bode, J. P. Ostriker, and G. Xu, "The Tree Particle-Mesh N-Body Gravity Solver," *Astrophys. J. Supp.*, vol. 128, pp. 561–569, Jun. 2000.
- [20] J. S. Bagla, "TreePM: A Code for Cosmological N-Body Simulations," *Journal of Astrophysics and Astronomy*, vol. 23, pp. 185–196, Dec. 2002.
- [21] J. Dubinski, J. Kim, C. Park, and R. Humble, "GOTPM: a parallel hybrid particle-mesh treecode," *New Astronomy*, vol. 9, pp. 111–126, Feb. 2004.
- [22] V. Springel, "The cosmological simulation code GADGET-2," *Mon. Not. R. Astron. Soc.*, vol. 364, pp. 1105–1134, Dec. 2005.
- [23] K. Yoshikawa and T. Fukushima, "PPPM and TreePM Methods on GRAPE Systems for Cosmological N-Body Simulations," *Publ. of the Astron. Society of Japan*, vol. 57, pp. 849–860, Dec. 2005.
- [24] T. Ishiyama, T. Fukushima, and J. Makino, "GreeM: Massively Parallel TreePM Code for Large Cosmological N-body Simulations," *Publ. of the Astron. Society of Japan*, vol. 61, pp. 1319–1330, Dec. 2009.
- [25] V. Springel, S. D. M. White, A. Jenkins, C. S. Frenk, N. Yoshida, L. Gao, J. Navarro, R. Thacker, D. Croton, J. Helly, J. A. Peacock, S. Cole, P. Thomas, H. Couchman, A. Evrard, J. Colberg, and F. Pearce, "Simulations of the formation, evolution and clustering of galaxies and quasars," *Nature*, vol. 435, pp. 629–636, Jun. 2005.
- [26] T. Ishiyama, T. Fukushima, and J. Makino, "Variation of the Subhalo Abundance in Dark Matter Halos," *Astrophys. J.*, vol. 696, pp. 2115–2125, May 2009.
- [27] A. A. Abdo, M. Ackermann, M. Ajello, W. B. Atwood, M. Axelsson, L. Baldini, J. Ballet, G. Barbiellini, D. Bastieri, M. Battelino, B. M. Baughman, E. D. Bloom, G. Bogaert, E. Bonamente, and A. W. Borgland, "Measurement of the Cosmic Ray  $e^+ + e^-$  Spectrum from 20 GeV to 1 TeV with the Fermi Large Area Telescope," *Physical Review Letters*, vol. 102, no. 18, pp. 181 101–, May 2009.
- [28] T. Ishiyama, J. Makino, and T. Ebisuzaki, "Gamma-ray Signal from Earth-mass Dark Matter Microhalos," *Astrophys. J. Lett.*, vol. 723, pp. L195–L200, Nov. 2010.
- [29] K. P. Zybun, M. I. Vysotsky, and A. V. Gurevich, "The fluctuation spectrum cut-off in a neutralino dark matter scenario," *Physics Letters A*, vol. 260, pp. 262–268, Sep. 1999.
- [30] V. Berezhinsky, V. Dokuchaev, and Y. Eroshenko, "Small-scale clumps in the galactic halo and dark matter annihilation," *Phys. Rev. D*, vol. 68, no. 10, pp. 103 003–, Nov. 2003.
- [31] J. Makino, "A Fast Parallel Treecode with GRAPE," *Publ. of the Astron. Society of Japan*, vol. 56, pp. 521–531, Jun. 2004.
- [32] D. Blackston and T. Suel, "Highly portable and efficient implementations of parallel adaptive n-body methods," in *Proceedings of the 1997 ACM/IEEE conference on Supercomputing (CDROM)*, ser. Supercomputing '97. New York, NY, USA: ACM, 1997, pp. 1–20. [Online]. Available: <http://doi.acm.org/10.1145/509593.509597>
- [33] K. Nitadori, J. Makino, and P. Hut, "Performance tuning of N-body codes on modern microprocessors: I. Direct integration with a hermite scheme on x86\_64 architecture," *New Astronomy*, vol. 12, pp. 169–181, Dec. 2006.
- [34] A. Tanikawa, K. Yoshikawa, T. Okamoto, and K. Nitadori, "N-body simulation for self-gravitating collisional systems with a new SIMD instruction set extension to the x86 architecture, Advanced Vector eXtensions," *New Astronomy*, vol. 17, pp. 82–92, Feb. 2012.
- [35] A. Tanikawa, K. Yoshikawa, K. Nitadori, and T. Okamoto, "Phantom-GRAPE: numerical software library to accelerate collisionless N-body simulation with SIMD instruction set on x86 architecture," *ArXiv e-prints*, Mar. 2012.
- [36] A. Kawai, T. Fukushima, J. Makino, and M. Taiji, "GRAPE-5: A Special-Purpose Computer for N-Body Simulations," *Publ. of the Astron. Society of Japan*, vol. 52, pp. 659–676, Aug. 2000.
- [37] A. M. Green, S. Hofmann, and D. J. Schwarz, "The power spectrum of SUSY-CDM on subgalactic scales," *Mon. Not. R. Astron. Soc.*, vol. 353, pp. L23–L27, Sep. 2004.
- [38] E. Komatsu, K. M. Smith, J. Dunkley, C. L. Bennett, B. Gold, G. Hinshaw, N. Jarosik, D. Larson, M. R. Nolta, L. Page, D. N. Spergel, M. Halpern, R. S. Hill, A. Kogut, M. Limon, S. S. Meyer, N. Odegard, G. S. Tucker, J. L. Weiland, E. Wollack, and E. L. Wright, "Seven-year Wilkinson Microwave Anisotropy Probe (WMAP) Observations: Cosmological Interpretation," *Astrophys. J. Supp.*, vol. 192, p. 18, Feb. 2011.
- [39] R. D. Skeel and J. J. Biesiadecki, "Symplectic integration with variable stepsize," *Ann. Numer. Math.*, 1994.
- [40] M. J. Duncan, H. F. Levison, and M. H. Lee, "A Multiple Time Step Symplectic Algorithm for Integrating Close Encounters," *Astron. J.*, vol. 116, pp. 2067–2077, Oct. 1998.
- [41] Y. Hasegawa, J.-I. Iwata, M. Tsuji, D. Takahashi, A. Oshiyama, K. Minami, T. Boku, F. Shoji, A. Uno, M. Kurokawa, H. Inoue, I. Miyoshi, and M. Yokokawa, "First-principles calculations of electron states of a silicon nanowire with 100,000 atoms on the k computer," in *Proceedings of 2011 International Conference for High Performance Computing, Networking, Storage and Analysis*, ser. SC '11. New York, NY, USA: ACM, 2011, pp. 1:1–1:11. [Online]. Available: <http://doi.acm.org/10.1145/2063384.2063386>